Supporting Information

Synergistic catalysis at in situ-formed Pt-NiOOH nanodot interfaces for highly efficient ammonia borane hydrolysis

Shuo Zhang,[a] Yao Chen,*[a] Zhenbo Xu,[a] Keju Sun,*[b] Xin Xiao,[c] Xiaolei Sun,[d] Yuanyuan Li,[e] Jiong Zhao,[f] Ding Chen,[a] Qiang Xu*[c]

[a] The State Key Laboratory of Refractories and Metallurgy, Faculty of Materials, Wuhan University of Science and Technology, Wuhan 430081, China. Email: y.chen@wust.edu.cn

[b] Hebei Key Laboratory of Applied Chemistry, School of Environmental and Chemical Engineering, Yanshan University, 438 Hebei Avenue, Qinhuangdao 066004, China. Email: kjsun@ysu.edu.cn

[c] Southern University of Science and Technology, Shenzhen, 518055, China. Email: xuq@sustech.edu.cn

[d] School of Materials Science and Engineering, Nankai University, Tianjin 300350, China.

[e] Analysis & Testing Center of Wuhan University of Science and Technology, Wuhan 430081, China.

[f] Department of Applied Physics, The Hong Kong Polytechnic University, Kowloon, Hong Kong, China.

Experimental

Chemicals

Natural graphite (Alfa Aesar Chemical Co. Ltd.), sodium nitrate ($NaNO_3$, AR, Sinopharm Chemical Reagent Co. Ltd.), sulfuric acid (H_2SO_4, 98%, Sinopharm Chemical Reagent Co. Ltd.), potassium permanganate ($KMnO_4$, AR, Xilong Scientific Co. Ltd.), hydrochloric acid (HCl, 36%, Sinopharm Chemical Reagent Co. Ltd.), hydrogen peroxide (H_2O_2, 30%, Sinopharm Chemical Reagent Co. Ltd.), potassium tetrachloroplatinate (II) (K_2PtCl_4, AR, Merck Sigma-Aldrich), nickel(II) chloride hexahydrate ($NiCl_2 \cdot 6H_2O$, AR, Sinopharm Chemical Reagent Co. Ltd.), N,N-Dimethylformamide (DMF, C_3H_7NO, 99.5%, Sinopharm Chemical Reagent Co. Ltd.), sodium hydroborate ($NaBH_4$, 98%, Sinopharm Chemical Reagent Co. Ltd.), ammonia borane (AB, NH_3BH_3, 98%, Anhui Senrise Technology Co. Ltd.) were used as raw materials.

Preparation

Preparation of GO: 2 g of natural graphite, 2 g of $NaNO_3$ and 92 mL of H_2SO_4 were mixed and stirred in an ice bath at −1 to −2 °C for 19 h. Next, 12 g of $KMnO_4$ was slowly added into the above mixture. After removing the ice bath, the resulting mixture was stirred at room temperature for 4 h. Following this, 184 mL of water was added dropwise, and the resulting suspension was stirred in a 98 °C water bath for 30 min. Then, 40 mL of H_2O_2 and 400 mL of water (60 °C) were added and stirred for 10 min. The resulting mixture was centrifuged and washed with concentrated HCl with stirring for 10 min. min. The product was further washed with water by centrifugation until the volume of the GO no longer expanded. At last, the slurry was transferred to a petri dish and dried at 60 °C for 48 h to obtain GO sheets.

Preparation of Pt-$Ni(OH)_x$/RGO-X: GO colloids with 2 $mg \cdot mL^{-1}$ was formed by mixing solid GO with deionized water and sonicating at 60 W for 4.5 h. Then, 0.01 mmol of K_2PtCl_4 and X mmol of $NiCl_2 \cdot 6H_2O$ (X = 0.03, 0.06, 0.09, 0.12 or 0.15) in 10 mL of water was added into 10 mL of the GO colloids and refluxed at 140 °C in an oil bath for 10 min. After adding 20 mL of DMF, the mixed liquid was continued to be stirred in the oil bath for 5 h. Finally, a series of Pt-$Ni(OH)_x$/RGO-X catalysts were obtained by centrifugation and washing with ethanol and water.

Preparation of $Ni(OH)_x$/RGO: The preparation of $Ni(OH)_x$/RGO was similar to the method for Pt-$Ni(OH)_x$/RGO-0.12 but without adding K_2PtCl_4 into the solution.

Preparation of Pt/RGO: Pt/RGO was synthesized by a similar method as for Pt-$Ni(OH)_x$/RGO-0.12 but without adding $NiCl_2 \cdot 6H_2O$ into the solution.

Preparation of Pt/RGO-$NaBH_4$: 0.01 mmol K_2PtCl_4 solution was dispersed in 10 mL of water. Then the metal precursor solution was mixed with 2 $mg \cdot mL^{-1}$, 10 mL of GO colloid, followed by the addition of 20 mL of water. The mixture was stirred at room temperature for 10 min. Subsequently, 0.03 g of $NaBH_4$ dissolved in 0.5 mL of water was poured into the mixture quickly, stirring for 20 min until no bubbles were generated. The resulting product was collected through vacuum filtration and washing, which was denoted as the Pt/RGO-$NaBH_4$ catalyst.

Preparation of Pt/RGO-$NaBH_4$-ST: The Pt/RGO-$NaBH_4$ catalyst was redispersed in 20 mL of water and stirred for 10 minutes in an oil bath at 140 °C. After adding 20 mL of DMF, the mixture was refluxed for 5 h. The solid product was washed by vacuum filtration with ethanol and water to obtain Pt/RGO-$NaBH_4$-ST.

Characterization

Powder X-ray diffraction (XRD) studies were performed on a SmartLab SE (Cu Ka radiation, λ = 1.5406 Å, Rigaku, Tokyo, Japan). Morphology and compositional analyses were conducted using transmission electron microscopy (TEM, JEMF200, JEOL, Tokyo, Japan) with energy-dispersive X-ray spectroscopy (EDS). X-ray photoelectron spectroscopy (XPS) was performed on a Thermo Fisher Scientific (Al Kα radiation, K-Alpha, USA). Inductively coupled plasma optical emission spectrometer (ICP-MS) was carried out in Agilent 7800 (Agilent, USA). Raman spectroscopy was used to characterize the structure of the materials utilizing HR Evolution (LabRam HR Evolution, Thermo Fischer DXR) with a laser with a wavelength of 532 nm.

Catalytic performance

The as-prepared catalyst loaded in a two-neck flask was dispersed in water to form 5 mL suspension. 2 mmol of AB dissolved in 2 mL of water was quickly injected into the two-neck flask using a syringe to initiate the catalytic reaction in a water bath at 303 K if without other specification. The volume of hydrogen produced was recorded every 15 s until no more bubbles were formed. Similar experiments were carried out by varying the concentration of AB or dosage of the catalyst. To test the recyclability of the catalyst, the catalyst was collected after the AB hydrolysis reaction by once centrifugation with another 6 mL water, and then redispersed in water for the next cycle.

Calculation of kinetics

The turnover frequency (TOF) of the Pt-based catalyst is calculated using Equation S1:

$$TOF = \frac{pV_{H_2}}{n_{Pt}RTt} = \frac{n_{H_2}}{n_{Pt} \times t} \quad \text{(S1)}$$

where n_{H2} is the number of moles of H_2 produced, n_{Pt} is the total number of moles of Pt in the catalyst, and t is the reaction time, R is the molar gas constant, and T is the thermodynamic temperature.

To study the reaction kinetics, the hydrolysis of AB was investigated at 298, 303, 308 and 313 K, and the activation energy (E_a) can be determined using Arrhenius Equation S2:

$$lnTOF = lnA - \frac{E_a}{RT} \quad \text{(S2)}$$

where A is the pre-exponential factor.

Assuming that Pt nanodots are homogeneous spheres with average size as diameter (D), Equation S3 and S4 express the surface area (A) and volume (V) of catalysts. As the reaction rate (v) is in direct proportion to surface area of catalysts, hence TOF is in direct proportion to the ratio of surface area to molar amount (n) of catalysts, shown in Equation S5. Therefore, the relationship between TOF and D was deduced by Equation S6.

$$A = N\pi D^2 \quad \text{(S3)}$$

$$V = \frac{N}{6}\pi D^3 \quad \text{(S4)}$$

$$TOF = \frac{v}{n} \propto \frac{A}{n} = \frac{AM}{\rho V} \quad \text{(S5)}$$

$$TOF \propto \frac{1}{D} \quad \text{(S6)}$$

where N is particle numbers, M is molar mass, ρ is density.

DFT calculation

Density Functional Theory (DFT) calculations were performed using the Vienna Ab-initio Simulation Package (VASP).[1] The Perdew-Burke-Ernzerhof (PBE) exchange-correlation functional[2] was employed in conjunction with the Projector Augmented Wave (PAW) method.[3] To account for van der Waals (vdW) interactions, we utilized the DFT-D3 functional with Becke-Johnson (BJ) damping.[4] For accurate treatment of the strongly correlated 3d orbitals of Ni, DFT + U calculations were conducted, applying a Hubbard U correction of 5.5 eV.[5] In the lattice constant calculations, a plane-wave cutoff energy of 600 eV was used, while a cutoff of 400 eV was employed for surface adsorption and reaction calculations. All calculations considered spin polarization and underwent geometric optimization until the residual forces on each atom were below 0.02 $eV \cdot Å^{-1}$. The computed lattice constant for pure Pt was found to be 3.936 Å, while for NiOOH, the lattice parameters were a = b = 2.99 Å and c = 4.52 Å, which is consistent with other simulation values (a = b = 2.97 Å, c = 4.54 Å).[6]

To simulate the dissociation reactions of water and AB on the Pt surface, we constructed a slab Pt-model of a 4×4 Pt(111) surface composed of four layers, with a vacuum height of 15 Å. During the geometric optimization process, the bottom two layers were fixed, while the top two layers and the adsorbates were allowed to relax. For the Pt/NiOOH interface, we established a Pt-NOOH model comprising a two-layer

2×4 NiOOH (001) surface and a Pt_4 cluster, with the lower layer of NiOOH fixed in its bulk structure, while the upper layer, Pt_4 cluster, and adsorbates were allowed to relax. For all surface calculations, a 3×3×1 Monkhorst-Pack k-point mesh was employed. The transition state search was conducted using the force-reversed method,[7] and the identified transition states were confirmed through frequency calculations, which indicated the presence of only one imaginary frequency.

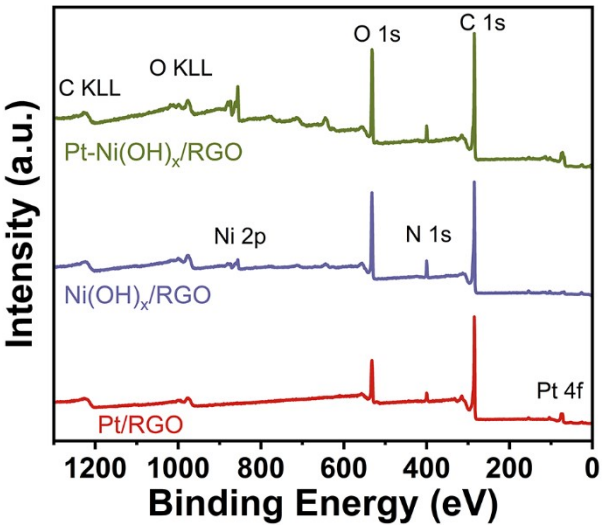

Fig. S1. XPS survey spectra of Pt/RGO, $Ni(OH)_x$/RGO and Pt-$Ni(OH)_x$/RGO.

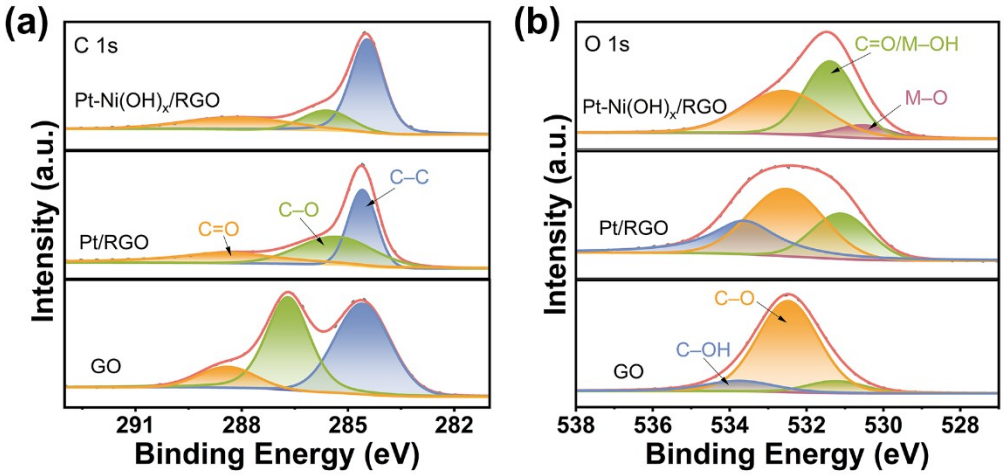

Fig. S2. High-resolution (a) C 1s and (b) O 1s XPS spectra of GO, Pt/RGO and Pt-$Ni(OH)_x$/RGO.

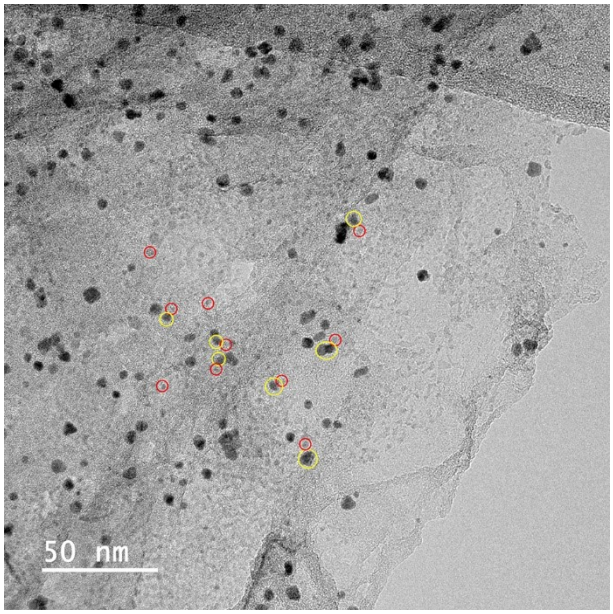

Fig. S3. TEM image of Pt-Ni(OH)$_x$/RGO, where Pt and Ni(OH)$_x$ indicated by yellow and red circles, respectively.

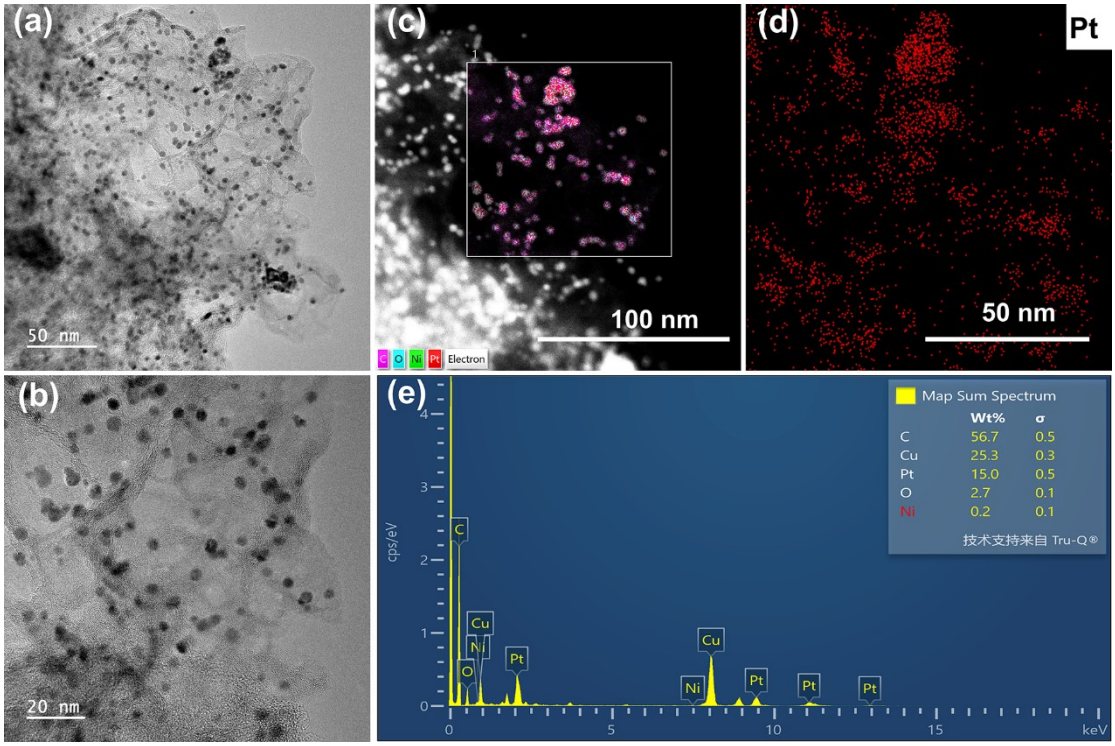

Fig. S4. TEM images at (a) low and (b) high magnifications, (c) HAADF image, (d) EDS mapping of Pt, (e) EDS spectrum in selected frame in (c) of acid treated Pt-Ni(OH)$_x$/RGO.

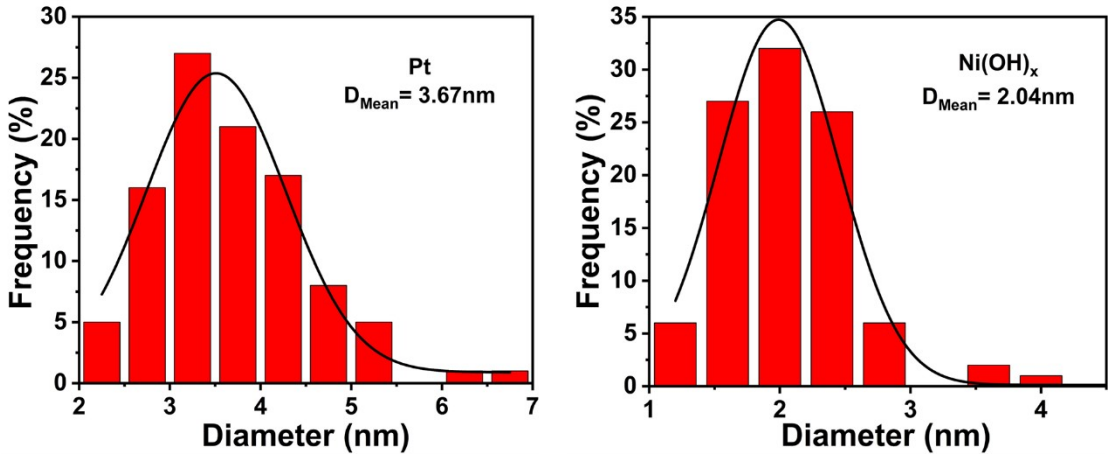

Fig. S5. Size distribution of Pt and $Ni(OH)_x$ nanodots in Pt-$Ni(OH)_x$/RGO.

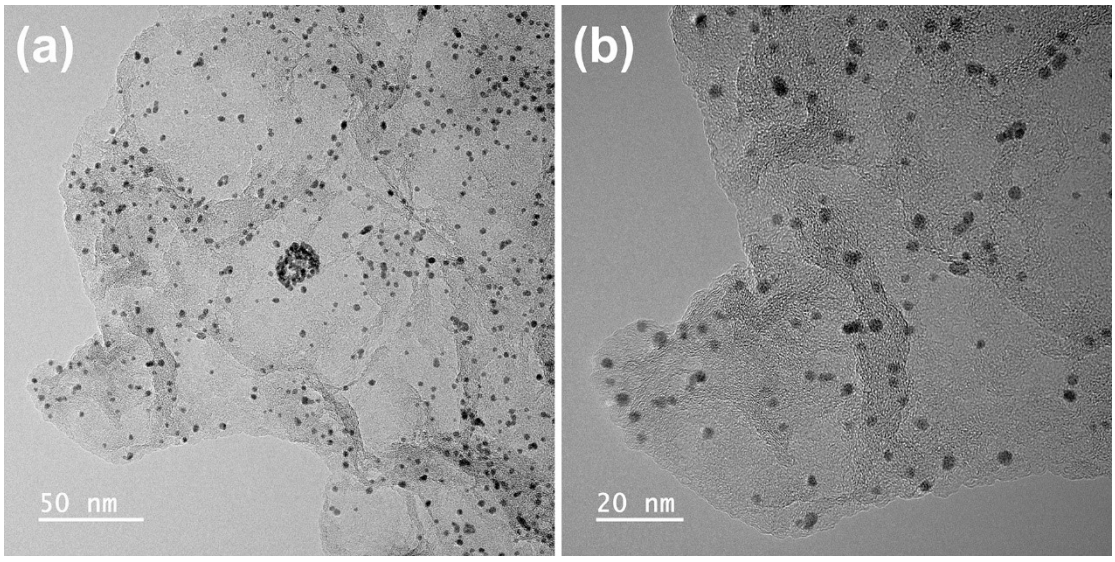

Fig. S6. TEM images of Pt/RGO at (a) low and (b) high magnifications.

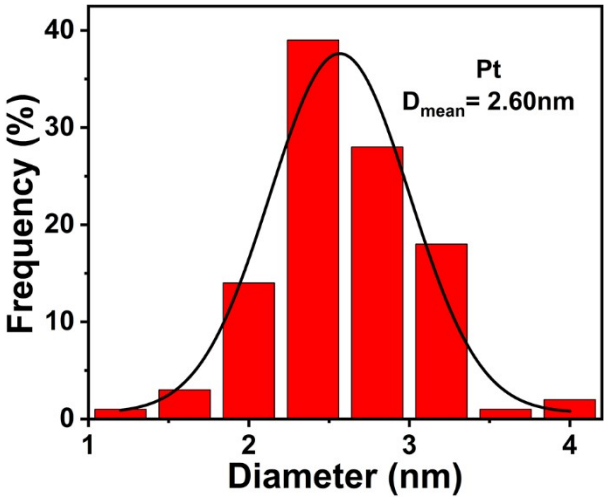

Fig. S7. Size distribution of Pt nanodots in Pt/RGO.

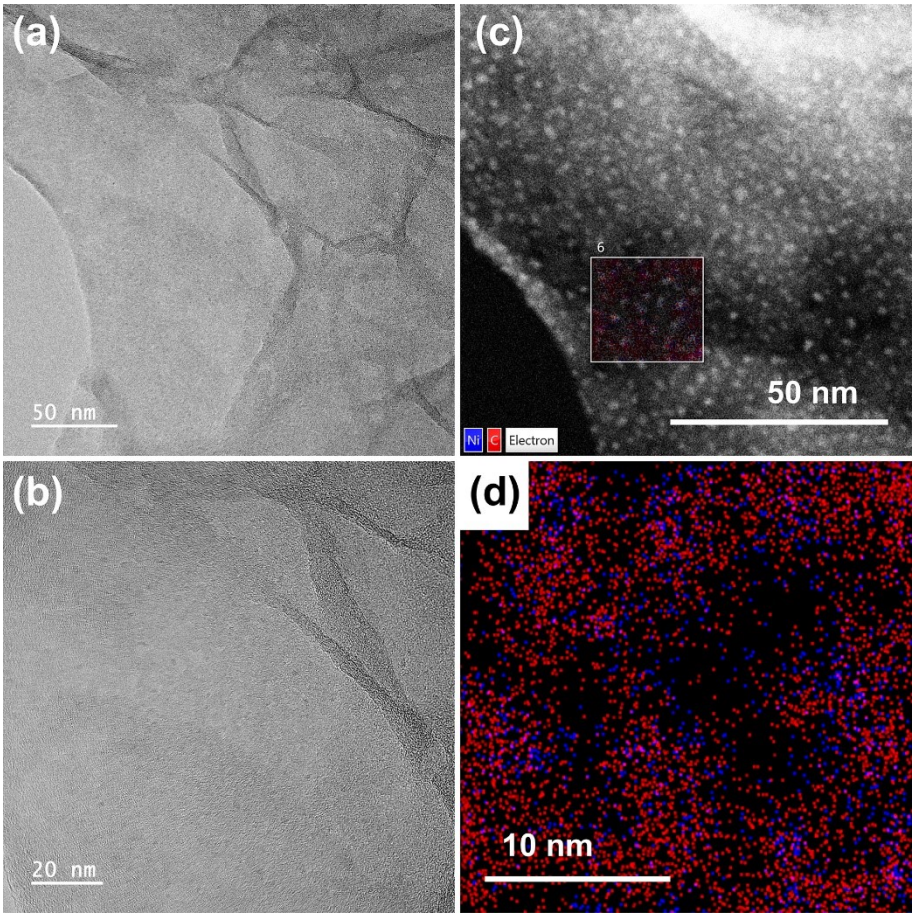

Fig. S8. TEM images at (a) low and (b) high magnifications, (c) HAADF image, (d) overlapped EDS mapping images of C and Ni in selected frame in (c) of $Ni(OH)_x$/RGO.

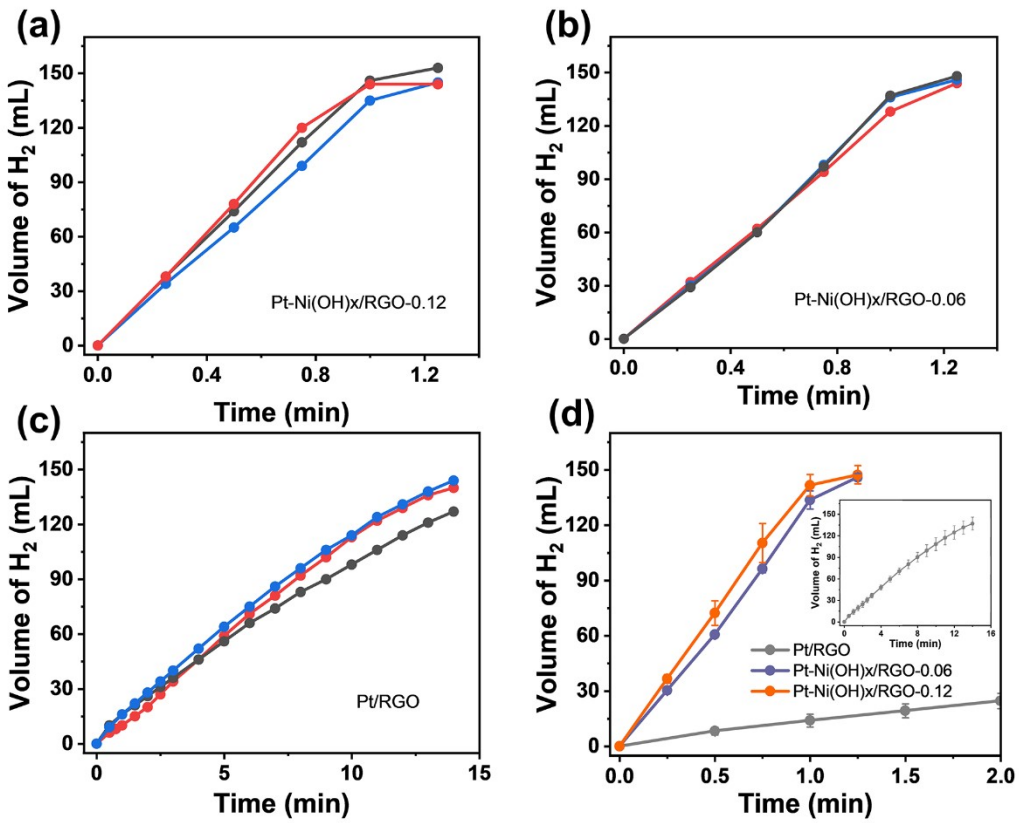

Fig. S9. Hydrogen evolution rates from AB hydrolysis over (a) Pt-Ni(OH)$_x$/RGO-0.12, (b) Pt-Ni(OH)$_x$/RGO-0.06, (c) Pt/RGO with triplicate data and (d) Pt-Ni(OH)$_x$/RGO-0.12, Pt-Ni(OH)$_x$/RGO-0.06 and inset (d) Pt/RGO with error bars, data corresponding to red curves adopted in Fig. 3a.

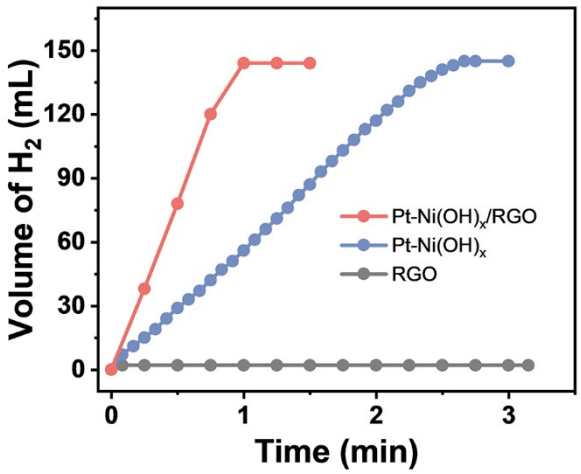

Fig. S10. Hydrogen evolution rates from AB hydrolysis over Pt-Ni(OH)$_x$/RGO, Pt-Ni(OH)$_x$ and RGO at 303 K**.**

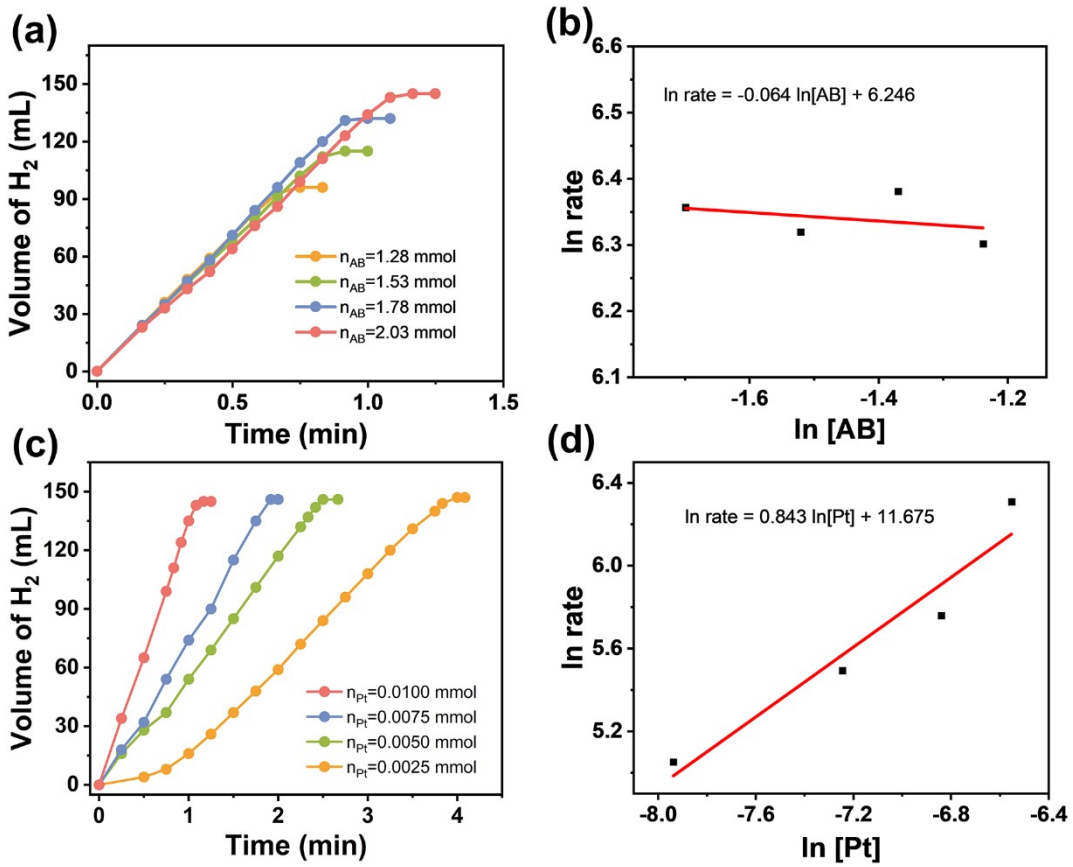

Fig. S11. (a) Hydrogen evolution rates from AB hydrolysis over Pt-Ni(OH)$_x$/RGO with various AB concentrations and (b) corresponding logarithmic plot of rate versus AB concentration, (c) hydrogen evolution rates from AB hydrolysis over various Pt-Ni(OH)$_x$/RGO dosage and (d) corresponding logarithmic plot of rate versus Pt concentration.

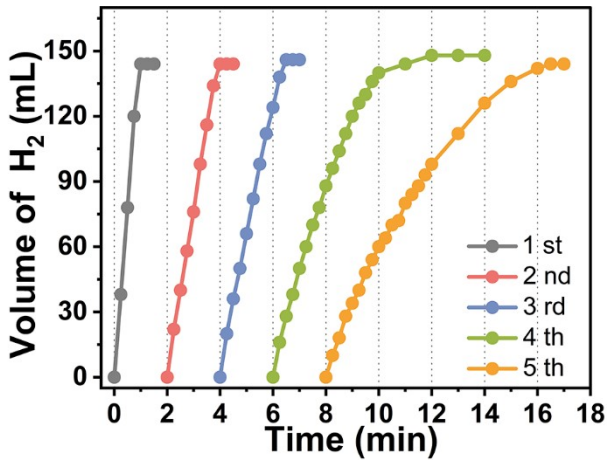

Fig. S12. Stability test of Pt-Ni(OH)$_x$/RGO.

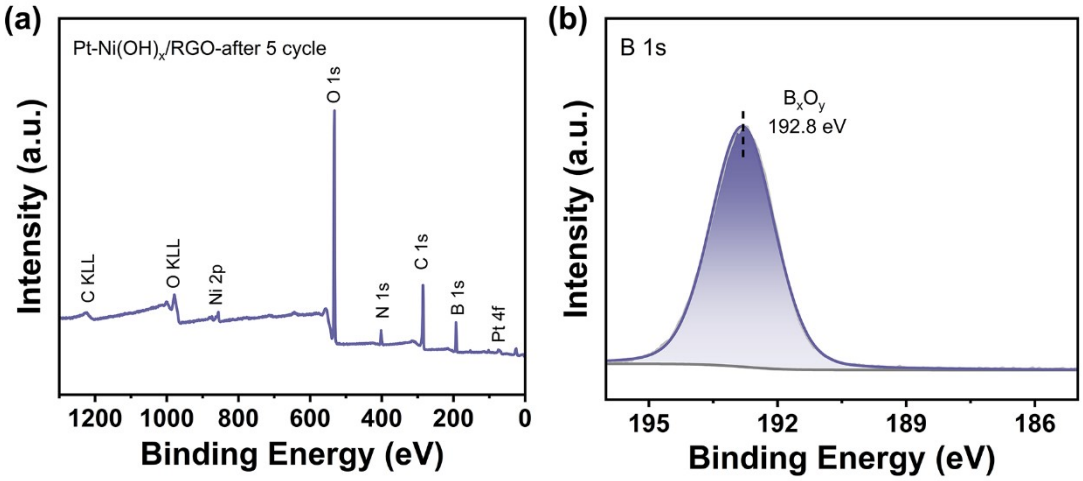

Fig. S13. XPS (a) survey and (b) B 1s spectra of Pt-Ni(OH)$_x$/RGO after five cycles.

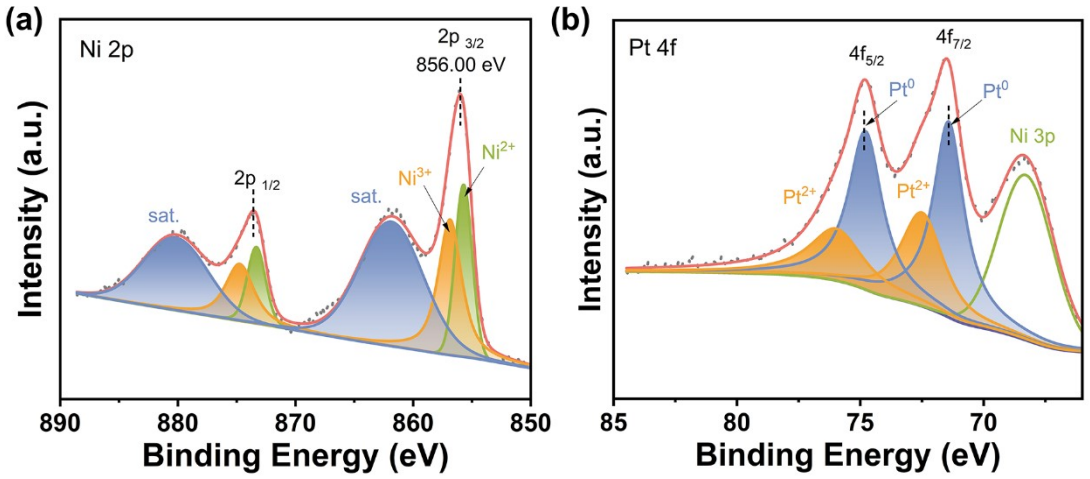

Fig. S14. XPS (a) Ni 2p and (b) Pt 4f spectra of Pt-Ni(OH)$_x$/RGO after AB hydrolysis.

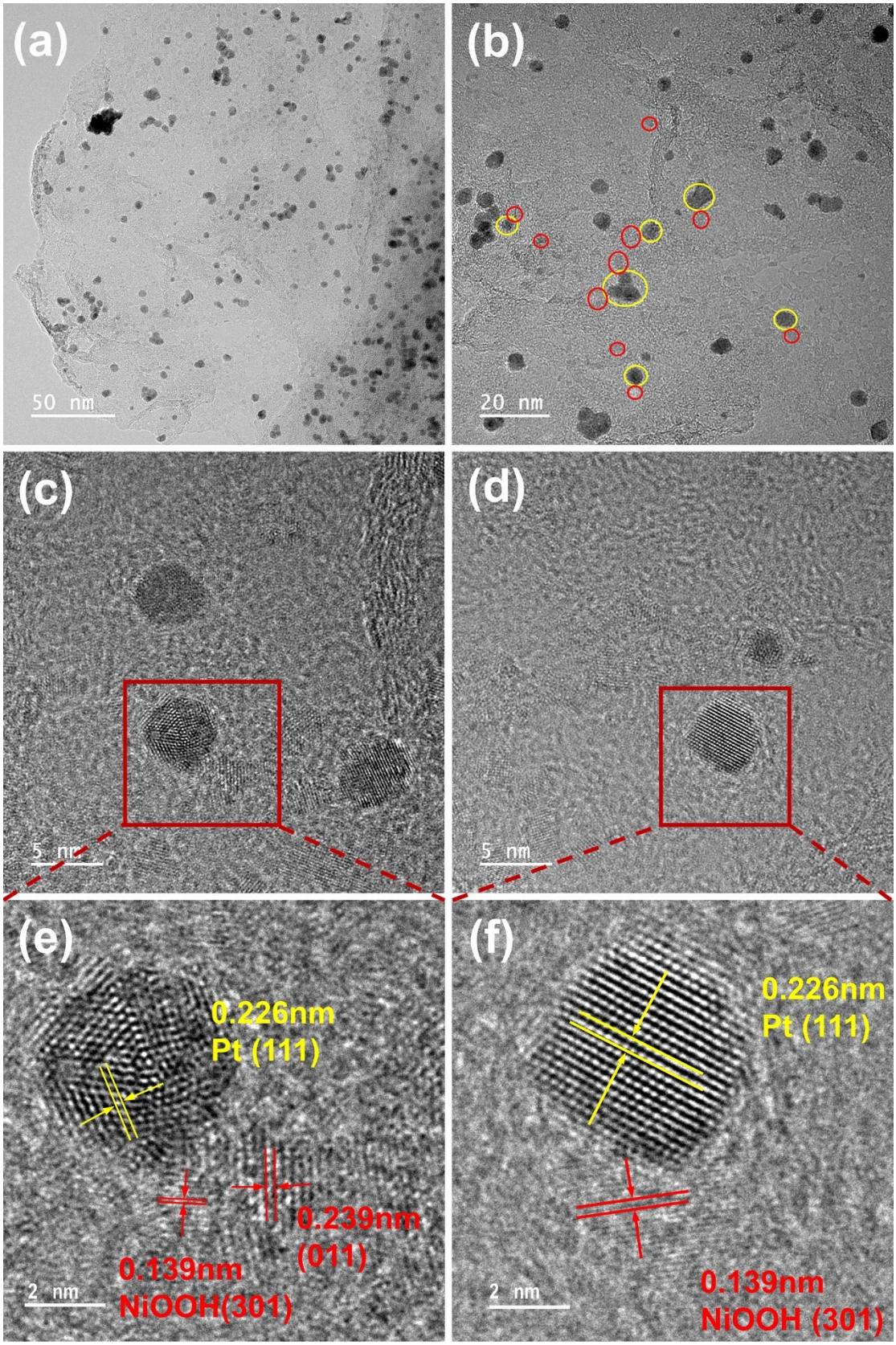

Fig. S15. (a-e) TEM images of Pt-$Ni(OH)_x$/RGO after AB hydrolysis, where Pt and $Ni(OH)_x$ indicated by yellow and red circles, respectively.

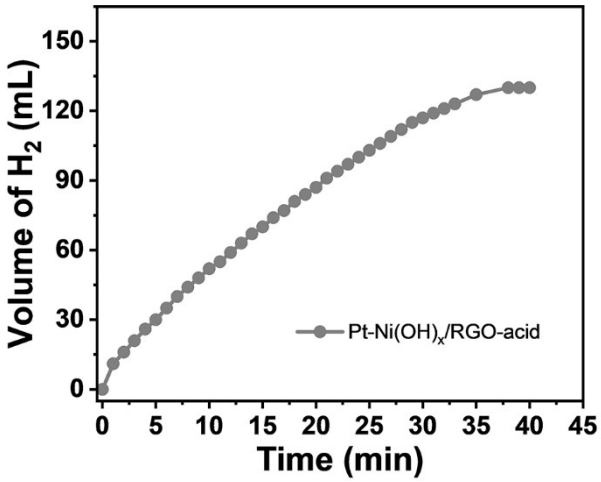

Fig. S16. Hydrogen evolution rates from AB hydrolysis over acid-treated Pt-Ni(OH)$_x$/RGO at 303 K.

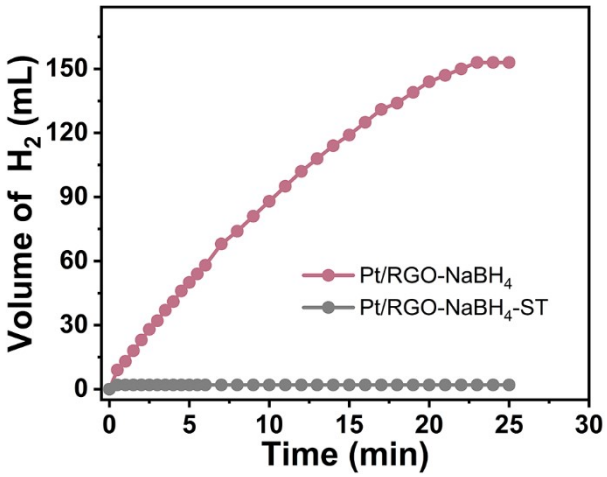

Fig. S17. Hydrogen evolution rates from AB hydrolysis over Pt/RGO-NaBH$_4$ and Pt/RGO-NaBH$_4$-ST at 303 K.

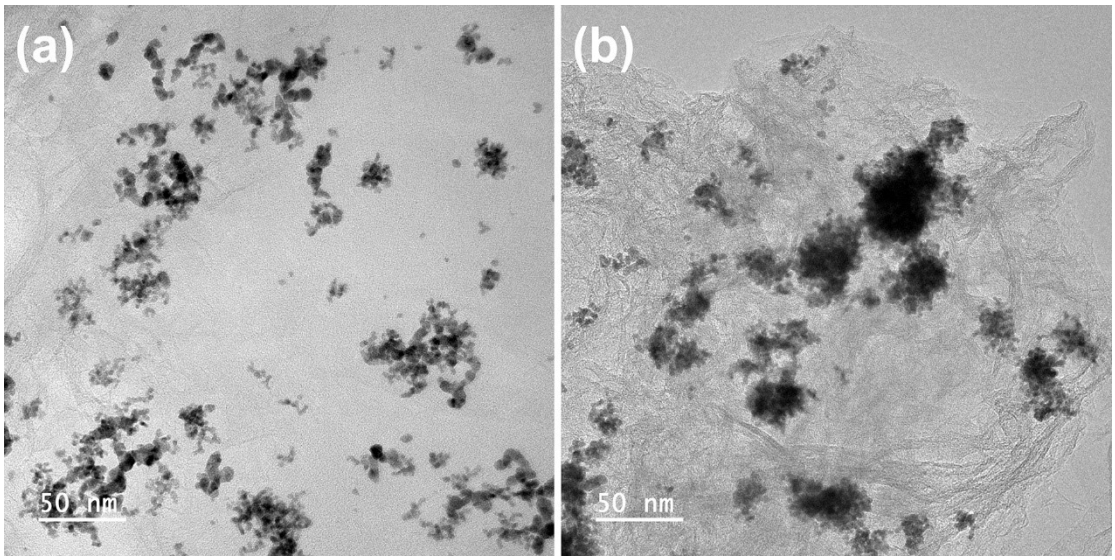

Fig. S18. TEM images of (a) Pt/RGO-$NaBH_4$ and (b) Pt/RGO-$NaBH_4$-ST.

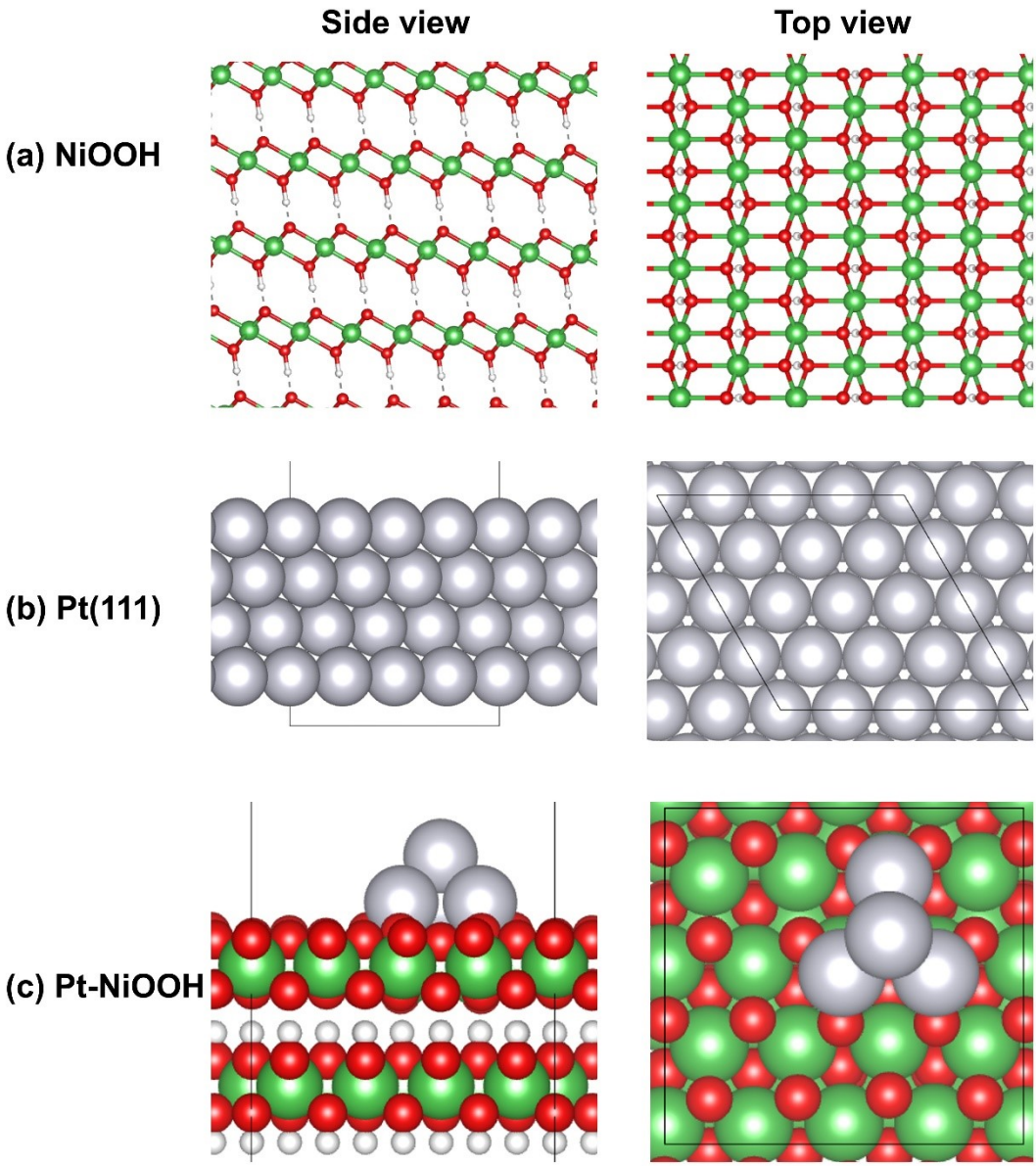

Fig. S19. Optimized structures of (a) NiOOH, (b) Pt(111) surface and (c) Pt-NiOOH.

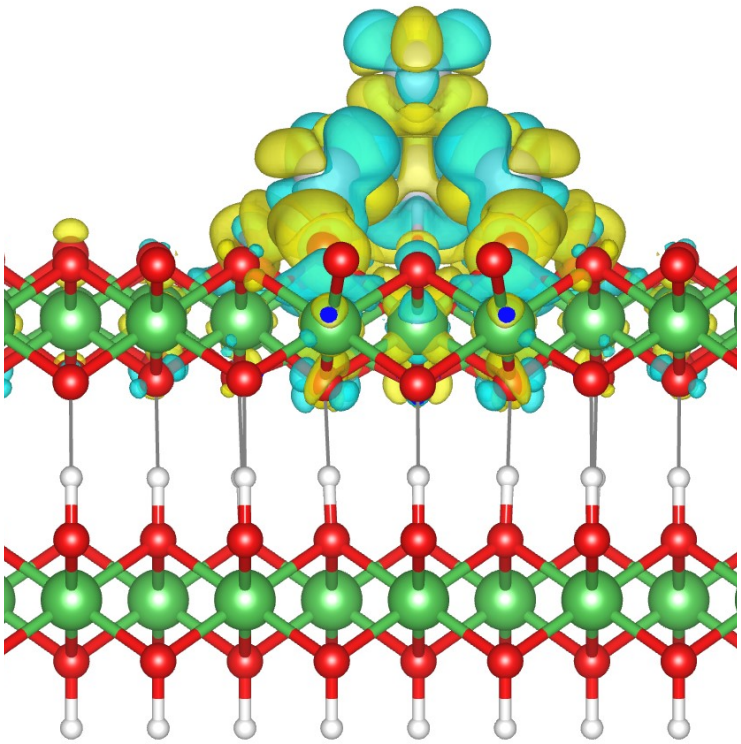

Fig. S20. Charge transfer from Pt_4 to NiOOH surface.

Table S1. ICP-MS of Pt-Ni$(OH)_x$/RGO and Pt/RGO.

Sample	**Pt (wt%)**	**Ni (wt%)**
Pt-Ni$(OH)_x$/RGO	0.67	12.54
Pt/RGO	1.02	—

Table S2. Costs of catalyst precursors.

	K_2PtCl_4	**$NiCl_2 \cdot 6H_2O$**
Unit cost (¥·g^{-1})	1352.34	0.25
Unit cost (¥·mmol^{-1})	0.56	5.9×10^{-5}
n of the same price (mmol)	1.06×10^{-4}	1

Table S3. Comparison of catalytic activities of Pt-Ni(OH)$_x$/RGO with those of other Pt-based catalysts for AB hydrolysis.

Catalyst	T (K)	E_a (kJ·mol^{-1})	TOF (mol$_{H_2}$·mol$_{Pt}^{-1}$·min^{-1})	Ref. [a]
Pt-Ni(OH)$_x$/RGO	303	50.3	17740	This work
	298		8138	
$Pt_{0.1\%}Co_{3\%}/TiO_2$	298	63.8	2250	27
Pt-PVP/SiO_2(M)	298	46.2	371	46
$PtNiO_xTVO$	298	59.3	618	47
PtNi@TiO_2	298	47.2	1055.2	48
RuPt−Ti	298	28.6	1293	49
Pt-Co/GQD	303	45.3	520	50
$Pt_0/CoFe_2O_4$	298	65	3628	51
5Pt/G1600-O_3-60	298	24.3	618.9	52
Pt_1Co_1/1	293	28.8	606	53
Ni_2Pt@ZiF-8	293	23.3	2222	54

[a], Ref. number is the same as those in main paper.

References

1. G. Kresse and J. Hafner, *Phys. Rev. B*, 1993, **48**, 13115-13118.
2. J. P. Perdew, K. Burke and M. Ernzerhof, *Phys. Rev. Lett.*, 1996, **77**, 3865-3868.
3. P. E. Blöchl, *Phys. Rev. B*, 1994, **50**, 17953-17979.
4. S. Grimme, S. Ehrlich and L. Goerigk, *J. Comput. Chem.*, 2011, **32**, 1456-1465.
5. E. R. Ylvisaker, W. E. Pickett and K. Koepernik, *Phys. Rev. B*, 2009, **79**, 035103.
6. A. J. Tkalych, K. Yu and E. A. Carter, *J. Phys. Chem. C*, 2015, **119**, 24315-24322.
7. K. Sun, Y. Zhao, H.-Y. Su and W.-X. Li, *Theor. Chem. Acc.*, 2012, **131**, 1118.